# Electronic Supplementary Information (ESI)

# New insights into Microbial-mediated synthesis of Au@biolayer Nanoparticles

Wenjing Liu,[a,b] Liying Wang,[a,b] Jin Wang,[c] Jingjing Du, [a,b] and Chuanyong Jing [a,b] *

[a]State Key Laboratory of Environmental Chemistry and Ecotoxicology, Research Center of Eco-Environmental Sciences, Chinese Academy of Sciences, Beijing 100085, China

[b]University of Chinese Academy of Sciences, Beijing 100049, China

[c]Department of Municipal & Environmental Engineering, School of Civil Engineering, Beijing Jiaotong University, Beijing 100044, China

- 23 Pages (including cover page)

## 1. Materials and Methods

### 1.1 Biogenic Au NPs in *Pantoea* sp. IMH

**1.1.1 Preparation of *Pantoea* sp. IMH.** *Pantoea* sp. IMH (JX861130) from our laboratory was maintained in Luria−Bertani (LB) broth. The organism was cultivated by inoculating freshly grown bacteria in a liquid medium with LB broth. The cultures were aerobically grown to late-log phase at 30 ºC. Cells were then harvested by centrifugation at 4000 *g* (Thermo scientific Heraeus multifuge X1R) for 3 min, washed with PBS buffer solution (pH 7.4) for three times, and used for Au NPs synthesis.

**1.1.2 biogenic Au NPs in *Pantoea* sp. IMH.** The harvested cells were re-suspended in PBS buffer (pH 7.4). Then, Au (III) was added to 10 mL of the above cells suspension and the final concentration of Au (III) reached to 1.8 mM. The mixture was incubated at 30 ºC. Control experiments without cells were also performed. After 12 h, the cells and nanoparticles were harvested by centrifugation at 4000 *g* for 10 min. All of the experiments were performed in triplicate.

### 1.2 Characterization of Au NPs by *Pantoea* sp. IMH

**1.2.1 UV-vis spectroscopy.** The cells suspension after nanoparticles synthesis was analyzed by UV-Vis spectroscopy (UV-2550 Shimadzu).

**1.2.2 High-resolution Transmission Electron Microscopy (HRTEM), electron diffraction (ED), and X-ray spectrometer (EDS).** The biogenic Au NPs were observed from the electron micrographs (HRTEM; Tecnai $G^2$ F20, FEI) at a voltage of 200 kV. Selected area electron diffraction (SAED) pattern was recorded from HRTEM images to obtain the crystal structure. The elemental analysis was confirmed through EDXA analysis.

**1.2.3 X-ray diffraction analysis.** The Au NPs were freeze-dried and prepared for X-ray powder diffraction (XRPD). The XRPD data were recorded on a Rigaku D/Max-2500 diffractometer at 40 kV, 100 mA using a Cu-target tube and a graphite monochromator. Scans were made in the 2θ range of 10° to 90° with a step size of 0.01° and a count time of 2 s per step. Analyses of the XRPD patterns were performed using the PDF-2 reference database from the International Center for Diffraction Data database.

**1.2.4 Field emission scanning electron microscopy.** The cells before and after nanoparticles synthesis were washed with phosphate buffer (pH 7.4) for three times, then fixed with 2.5% glutaraldehyde in phosphate buffer (pH 7.4) for 4h and fixed in 1% $OsO_4$ in phosphate buffer at 4 ºC for 4h after washing thrice with the 0.1 M phosphate buffer (pH 7.4). The fixed cells were dehydrated with graded ethanol (30-100%) series after washing thrice with the 0.1 M phosphate buffer (pH 7.4) again. Then the samples were immersed in isoamyl acetate twice for 15 min. And samples were dried according to a procedure called the Critical Point Drying (CPD). Finally, the

powder sample was mounted on aluminum stubs using a double-sticky tape and analyzed with field emission scanning electron microscopy (FESEM) with an Oxford energy dispersive X-rayspectroscopy (EDS) analyzer (SU 8020, Hitachi). The results were shown in Figure S1.

**1.3 Preparation of thin section samples for HRTEM observation.**

Cells before and after nanoparticles synthesis were thoroughly washed with phosphate buffer (pH 7.4), then fixed with 0.15% glutaraldehyde in phosphate buffer (pH 7.2) at 4 ºC for overnight. The fixed cells were dehydrated with graded ethanol (75-100%) series and embedded in resin. The samples were then thin sectioned (70 nm) in ultramicrotome using a diamond knife, and collected on a carbon coated copper grid. However, instead of staining ultrathin sections with uranyl acetate and lead citrate, electron scattering provided by the adsorbed metal ions and synthesized nanoparticles was acted as the contrasting agent. Localization of nanoparticles within the cell was observed from HRTEM.

**1.4 Biolayer characterization.**

**1.4.1 Separation of extracellular biogenic Au NPs.** Cells were firstly removed by centrifugation at 4000 *g* for 10 min from suspension after Au NPs synthesis. Then the extracellular biogenic Au NPs were harvested from the supernatant by centrifugation (13000 g for 30 min) followed by thoroughly washing in phosphate buffer (pH 7.4) to remove other substances from nanoparticles surface. Finally, the extracellular Au NPs were concentrated to 2 mL per 100 mL reaction solution.

**1.4.2 Identification of phospholipid.** The method of phospholipid extraction and detection was used as reported in a previous study.[1] The biogenic Au NPs were extracted with 50 mL of $CHCl_3$: $CH_3OH$: water (4:3:3) three times to isolate polar lipids in the organic phase. Then the phospholipid extract was evaporated by centrifugation under a vacuum. The Phospholipid extracts were infused into the TurboV electrospray source of a mass spectrometer model QTRAP® 4500 (AB SCIEX). ESI-MS/MS experiments were performed in the PC, PE, PS, PA, PI, PG with fast polarity switching (50 ms) and a scan rate of 200 Da/s. In the positive ion mode, PC can be identified by scanning for precursors of m/z 184, whereas PE, PG, PI and PA give the characteristic neutral losses of 141, 172, 277, and 98, respectively.

**1.4.3 Identification of protein.** The proteins bound with the nanoparticles were released from the nanoparticle surface by boiling with 1% SDS solution for 10 min. The supernatant was collected by centrifugation at 13000 *g* for 15 min. Then, the supernatant was subjected to SDS-PAGE electrophoresis. The SDS-PAGE gels were then sequentially and vertically cut with a razor blade, giving proteins separated in the all ranges. Each gel slice was further digested with trypsin. The tryptic digested peptide samples were analyzed by Nano LC-MS/MS (Fisher Scientific, USA) as described in

the previous study.[2] For protein identification, raw data files were converted to Mascot generic format (mgf) files and searched in the National Center for Biotechnology Information (NCBInr) database via Mascot Search (version 2.4, Matrix Science). Mascot search parameters included trypsin as the proteolytic enzyme with 1 missed cleavage. A minimal Mascot score of 25 and two different identified peptides were set for protein identity validation. The bioinformatics analysis was done according to the Gene Ontology (GO) annotations of identified proteins from the UniProt database (Universal Protein Resource, www.uniprot.org, UniProt release 2013_03).

**1.5 XPS analysis for extra- and intra-cellular Au NPs**

**1.5.1 Collection of extracellular and intracellular Au NPs.** The cells were incubated with 1.8 mM Au(III) for 12 h before the collection of the extracellular and intracellular Au NPs. To collect the Au NPs, the suspension was passed through a 0.45 μm membrane under vacuum, followed by repeated washing with Milli-Q water. Note that Au NPs with 10~50 nm diameter could readily pass through the membrane. Then, the extracellular Au NPs were harvested from the filtrate by centrifugation (13000 *g* for 30 min) followed by thoroughly washing in phosphate buffer (pH 7.4) to remove loosely attached substances from the NP surface.

After the removal of EPS and associated gold contents in the membrane, as mentioned in the EPS and membrane separation section, the cell pellets remaining on the filter membrane were disrupted by routine sonication on ice (Ultrasonic Homogenizer, SCIENTZ-IID, Φ6) at 950 W for 10 min with every 30s intervals. Then, the cell lysate was collected and resuspended to 100 mL water. The suspension was centrifuged at 350 *g* for 3 min and the precipitate in the bottom was removed. Then the suspension was centrifuged at 1000, 2500 *g* for 3 min, similar with previous 350 *g* centrifugation process. Each step was run in three replicates. Cell debris was mainly removed from the suspension. The intracellular biogenic Au NPs were harvested from the supernatant by centrifugation (13000 *g* for 30 min) followed by thoroughly washing in phosphate buffer (pH 7.4) to remove other substances from nanoparticles surface.

Bare Au NPs without any coating were purchased from Beijing DK Nanotechnology Inc. as a control sample.

**1.5.2 XPS Measurement.** XPS analysis was conducted for extracellular, intracellular, and bare Au samples. The samples were vacuum dried and ground to pass a 100 mesh sieve before XPS data collection with an ESCALab 220i-XL electron spectrometer from VG Scientific using 300 W Al Ka radiation. The base pressure was $3\times10^{-9}$ Pa. The binding energies were referenced to the C1s line at 284.8 eV from adventitious carbon. XPS data processing and peak fitting were performed using XPSPeak software package.

**1.6 Dynamic process of Au NP formation.**

**1.6.1 Quantifying the mass of Au NPs in microbial systems.** After cells incubation with 1.8 mM Au(III) for 12 h, the batch samples were analyzed to detect concentrations of Au(III) in whole system, culture medium, membrane, and cytoplasm.

**Whole system.** The bacterial suspension were prepared with routine sonication on ice (Ultrasonic Homogenizer, SCIENTZ-IID, Φ6) at 950 W (10 min with every 30s intervals) to disrupt cells and release all Au NPs.

**Medium(EPS).** The bacterial suspension was filtered through a 0.45 μm membrane under vacuum, followed by repeated washing with Milli-Q water. Note that Au NPs had particle sizes of 10~50 nm in diameter and could readily pass through the membrane. Then the concentrations of Au(III) and total Au in the filtrate as medium were analyzed.

**Membrane.** The filtered bacterial pellet was first resuspended in Milli-Q water and EPS associated on the cell membrane were extracted from the bacterial suspension using the sonication/centrifugation method, as mentioned in the EPS extraction section. The supernatant was filtered through a 0.45 μm membrane to remove unsettled cells. The filtered cells on the filter membrane were resuspended in Milli-Q water and filtered. Such a process was repeated at least 5 times to make sure that EPS and associated gold contents sorbed to cell membrane were completely washed out (verified by non-detectable gold content in the final filtrate after microwave digestion). The filtrates were collected and analyzed for the concentrations of Au in membrane location.

**Cytoplasm.** After the removal of EPS and associated gold contents in the membrane, the remaining cell pellets were disrupted by sonication as described in the whole system section. Then the cell lysate was collected and resuspended to 100 mL, then analyzed for the concentrations of Au in the cytoplasm.

**Au(III) separation, Microwave indestion and ICP-MS measurement.** The every fraction sample was added into Amicon centrifugal ultrafilter units (Ultra-15 3K, Millipore, cellulose membranes with 1-2 nm pore size), and subjected to centrifugation for 30 min at 8000 *g*. The Au(III) in the medium were concentrated in the filtrates, whereas Au NPs were remained in the cellulose membrane. Au(III) were quantified by ICP-MS (PerkinElmer NexION 350X). Before ICP-MS determination, the separated Au(III) and total Au samples were digested by microwave-assisted digestion (CEM Mars 5, Xpress, Matthews, NC) with a procedure. Briefly, 6 mL concentrated HCl and 2mL concentrated $HNO_3$ were added into the 2 mL samples and the mixture was irradiated at 140 °C (1600 W) for 10 min, followed by 190 °C (1600 W) for 30 min. After digestion, samples were diluted with water to 15 mL and stored at 4 °C for further analysis. By respective determining the total Au concentration (TAu) without ultrafiltration and the concentration of the Au(III) (Au(III)) in the filtrate after

ultrafiltration, the Au NPs concentration (Au NPs) was calculated as Au NPs = TAu – Au(III). Triplicate samples were run for the analysis of Au(III) at each fraction of microbial systems. The data were reported as the mean ± standard deviation.

**1.6.2 XANES-LCF Analysis.** The XANES spectra at the Au L-edge (eV) were collected at beamline 14W1 in the Shanghai Synchrotron Radiation Facility, China. An energy range of -200 to1000 eV from the L-edge of Au (11919 eV) was used to acquire the spectra. The spectra were analyzed using a linear combination fit in the Athena program in the IFEFFIT computer package.[3] The data processing and fitting approach are similar to that used in our previous study.[4]

**1.7 Extracellular mechanism: EPS role.**

**1.7.1 EPS extraction and Au NPs synthesis.** The bacteria were separated from the medium by centrifugation (6000 *g* at 4 ºC), followed by repeated washing with sterile water for three times. The bacteria were then suspended to 50% of the original volume. EPS was extracted from the bacterial suspension, as described in the literature.[5] The bacterial suspension was processed by ultrasound with an intensity of 2.7 W $cm^2$ at a frequency of 40 kHz at 4 ºC for 10 min, and then centrifuged at 12000 *g* at 4 ºC for 20 min to separate the cells. Then the supernatant was collected and filtered through a 0.45 μm membrane to remove unsettled cells. The filtrate (aqueous EPS) was stored at 4 ºC. To synthesize Au NPs, Au (III) was added to 10 mL of the above aqueous EPS and the final concentration of Au (III) reached to 1.8 mM. The mixture was incubated at 30 ºC for 12h. The aqueous EPS before and after Au(III) reaction were freeze-dried at −65 ºC for later FTIR experiment.

**Exopolysaccharides extraction method**. Exopolysaccharides were extracted from the aqueous EPS as described in the literature.[6] The EPS solution was added three fold volumes of 95% ethanol, and exopolysaccharides were precipitated. Then, the mixture was chilled at 4 ºC for 24 h. The resulting precipitates were recovered by centrifugation at 10000 *g* for 15 min. The precipitates were washed with 90% ethanol–water mixtures and freeze-dried at −65 ºC for later experiment.

**1.7.2 FTIR characterization.** Infrared spectra of EPS before and after nanoparticles synthesis were collected on Thermo-Nicolet Nexus 6700 FTIR spectrometer equipped with a liquid-nitrogen-cooled mercury−cadmium−telluride (MCT) detector. The pressed pellets were prepared by grinding the samples with KBr in a mortar at the ratio of 1:100 and analyzed over 256 scans with a resolution of 4 $cm^{-1}$.

**1.8 Intracellular mechanism: transcriptome analysis.**

**1.8.1 RNA Isolation and cDNA Synthesis.** The strain was cultivated by inoculating freshly grown bacteria in a liquid medium with LB broth. The cultures were aerobically grown to late-log phase at 30 ºC. Cells were then harvested by centrifugation at 4000 *g* for 3 min, washed with PBS buffer solution (pH 7.4) for three times. The harvested

cells were re-suspended in PBS buffer (pH 7.4). Then, Au (III) was added to the above cells suspension and the final concentration of Au (III) reached to 200 μM. The mixture was incubated at 30 ºC for 0, 10, 35 min to isolate total RNA. RNA isolation was carried out using Trizol reagent (TIANGEN, Beijing, China) according the manufactory's direction. The concentration and quality of total RNA was measured using NanoDrop 2000 (Thermo Scientific, USA). The isolated RNA was used for further transcriptome analysis and reverse transcription for cDNA synthesis. The reverse transcription was performed by PrimeScript RT reagent Kit with gDNA Eraser (Takara, Japan). The cDNA was stored at −80 ºC for further expression analysis.

**1.8.2 Transcriptome Analysis.** Transcriptome sequences are obtained from Illumina HiSeq 2000 sequencers.[7] All the high quality sequences were aligned against the reference genome with the spliced aligner TopHat. We used reads mapped to the genome to calculate every gene's expression in each sample. Then RPKM (Reads Per Kb per Million reads) was used to estimate expressions of genes so as to normalize the effects of different gene lengths and different total mapped reads among samples.[8] Differentially expressed genes (DEGs) were detected, as described in the literature.[9] P-value was used to test the statistical significance, and FDR (false discovery rate) was used to determine the threshold of P-value in multiple tests. Finally, the threshold with "FDR < = 0.050" and "absolute value of log2Ratio >= 10" was set to judge the significance of differences. We mapped all DEGs to GO terms in the database, calculating gene numbers for every term, then used hypergeometric test to find significantly enriched GO terms in DEGs comparing to the genome background.

**1.8.3 Quantitative Real Time PCR Verification.** To verify the transcriptome data, real time quantitative PCR assays were performed to analyze the relative expression levels of the several genes in the Au(III) treated cells for different induction time. Housekeeping gene (16S) was used as a reference gene to normalize mRNA expression of other related genes. Primer information is shown in Table S6. Every sample was run twice with three replicating. The quantification of target gene expression was based on a comparative cycle threshold (Ct) value. The expression level of each target gene was normalized to its reference gene 16s (Ct). The fold change of each gene was analyzed by the $2^{-\Delta\Delta Ct}$ method.[10]

## 2 Results and discussion

**Table S1**. List of bacteria that synthesize Au nanoparticles

| Bacteria | Size (nm)/Shape | Localization | Reference |
|---|---|---|---|

| | | | |
|---|---|---|---|
| *Bacillus subtilis* 168 | 5~25/ Octahedral | cell wall | [11] |
| *Plectonema boryanum* UTEX 485 | <10-25/ Cubic<br><10/ Octahedral platelets | Membrane vesicles<br>Intracellular | [12] |
| *Ralstonia metallidurans* | grains and nuggets | | [13] |
| *Rhodopseudomonas capsulate* | 10−400/ Spherical, triangular, nanoplates<br>10−30/ Spherical,<br>50−60/ nanowire | Extracellular | [14] |
| *Cupriavidus metallidurans* CH34 | particulate Au | Intra- and extracellular | [15] |
| *Brevibacterium casei* | 10–50/ spherical | Extracellular | [16] |
| *Shewanella algae* | 10-350/ Triangular, hexagonal | Periplasmic space, extracellular | [17] |
| *Synechocystis sp.* PCC 6803 | | intracytoplasmic membranes | [18] |
| *Shewanella oneidensis* MR-1 | ~5 /spherical | Intracellular<br>Extracellular | [19] |
| *Micrococcus luteus* | ~50/ spherical | Extracellular | [20] |
| *Geobacillus stearothermophilus* | ~12 /spherical | Extracellular | [21] |
| *Delftia acidovorans* | spherical<br>octahedral | | [22] |
| *Shewanella putrefaciens* CN32 | spherical | cell wall | [23] |
| *Escherichia coli* K12 | ~50/ nanoplates | Extracellular | [24] |
| *Spirulina platensis* | 6~10 | Extracellular | [25] |
| Sulfate-reducing bacteria | <10<br><25 | Intracellular<br>Extracellular | [26] |
| *Bacillus licheniformis* | 10~100/ Cubic | Extracellular | [27] |
| *Rhodobacter capsulatus* | | Plasma membrane | [28] |
| *Bacillus megatherium* D01 | 1.9±0.8/ Spherical | Extracellular | [29] |
| *Escherichia coli* DH5α | Spherical | Cell surface | [30] |
| *Lactobacillus sp.* | 20~50 /Hexagonal | Cell surface | [31] |

247

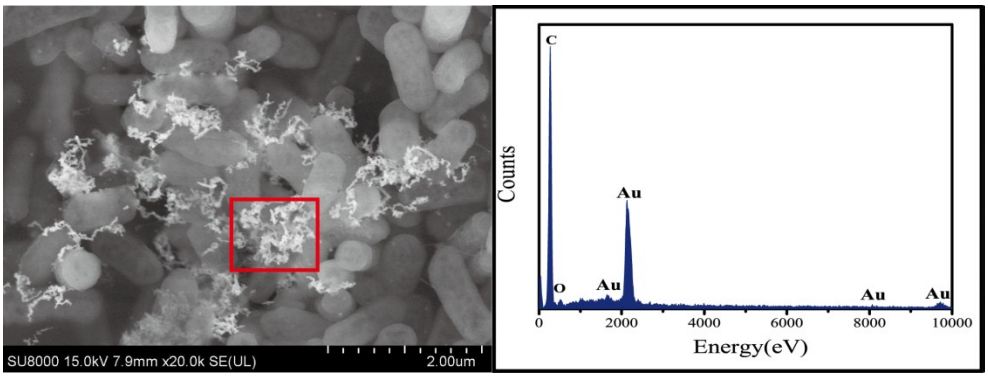


**Figure S1.** SEM image and EDS results show formation of biogenic Au NPs on the surface *Pantoea* sp. IMH.

**Table S2.** The mass of Au(III) and Au NPs in the extracellular medium (EPS), membrane, and cytoplasm.

| Au Con. (mg) | Whole | Medium(EPS) | Membrane | Cytoplasm |
|---|---|---|---|---|
| Total Au | 35.07 ± 0.12 | 25.02 ± 0.29 | 0.08 ± 0.00 | 9.85 ± 0.09 |
| Au(III) | 9.46 ± 0.22 | 7.68 ± 0.02 | 0.00 ± 0.00 | 1.58 ± 0.06 |
| Au NPs | 25.61 ± 0.24 | 17.34 ± 0.29 | 0.08 ± 0.00 | 8.27 ± 0.12 |

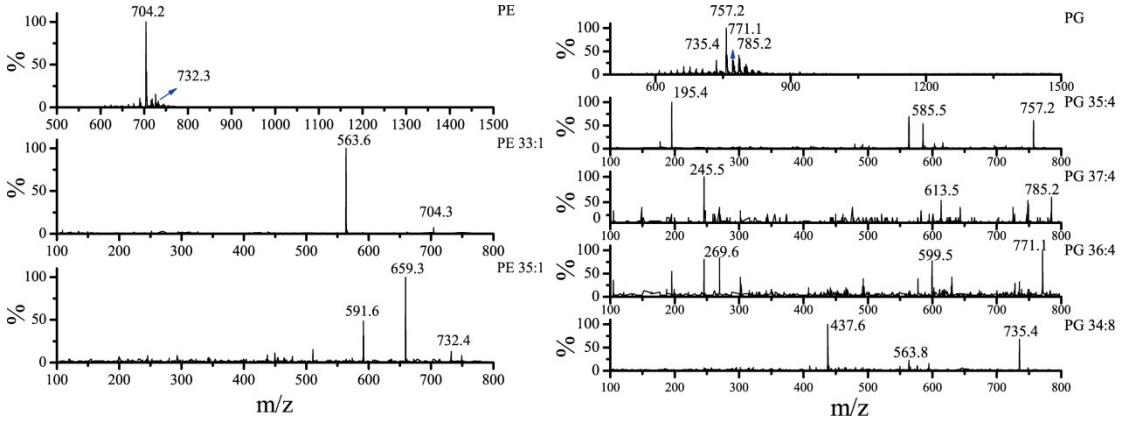


**Figure S2.** MS spectrum on phosphatidyl ethanolamine (PE) and phosphatidyl glycerol (PG) from biolayer

**Table S3**. Mass Measurements by Qtrap-MS for lipid identification (m/z).

| | M+H | Fragment | MW | Proposed lipid |
|---|---|---|---|---|
| PE-1 | 704.2 | 563.6(-PE) | 703.5 | PE 33:1 |

| | | | | |
|---|---|---|---|---|
| | | | | PE O-34:1 |
| PE-2 | 732.3 | 591.6(-PE) | 731.5 | PE 35:1 |
| | | | | PE O-36:1 |
| PG-1 | 757.2 | 585.5(-PG) | 756.5 | PG 35:4 |
| | | | | PG O-36:4 |
| PG-2 | 785.2 | 613.5(-PG) | 784.5 | PG 37:4 |
| | | | | PG O-38:4 |
| PG-3 | 771.1 | 599.5(-PG) | 770.5 | PG 36:4 |
| | | | | PG O-37:4 |
| PG-4 | 735.4 | 563.8(-PG) | 734.4 | PG 34:8 |
| | | | | PG O-35:4 |

**Table S4.** Proteins identified by LC-MS/MS

| Protein Name [32-34] | Accession no.[a] | Protein annotation | Mascot score | Calculated Mass(Da)[b] | Sequence coverage [c] | Identified peptides |
|---|---|---|---|---|---|---|
| Membrane Protein | gi\|687259738\|gb\|KGD82872.1\| | membrane protein [*Pantoea stewartii* subsp. indologenes] | 453 | 40677 | 9% | 3 |
| | gi\|671628669\|ref\|WP_031592851.1\| | membrane protein [*Pantoea agglomerans*] | 1109 | 41111 | 15% | 5 |
| Outer membrane protein | gi\|666372489\|gb\|KEY42626.1\| | outer membrane protein A [Pantoea *agglomerans*] | 103 | 38402 | 14% | 5 |
| | gi\|666372862\|gb\|KEY42999.1\| | outer membrane porin protein [*Pantoea agglomerans*] | 121 | 38989 | 5% | 7 |
| Lipoprotein | gi\|685439174\|gb\|KGB00005.1\| | major outer membrane lipoprotein Lpp [*Pantoea agglomerans*] | 191 | 8443 | 30% | 2 |
| | gi\|685440672\|gb\|KGB01503.1\| | outer membrane lipoprotein slyB [*Pantoea agglomerans*] | 78 | 15452 | 15% | 2 |
| | gi\|685441399\|gb\|KGB02227.1\| | maltose-binding periplasmic protein [*Pantoea agglomerans*] | 41 | 43033 | 2% | 2 |
| Maltoporin | gi\|691221133\|gb\|AIR84418.1\| | maltoporin [*Pantoea rwandensis*] | 157 | 48246 | 6% | 2 |

*a.* NCBInr database accession number.

*b.* Theoretical values for protein precursors obtained from the NCBI database (http://www.ncbi.nlm.nih.gov).

*c.* Percentage of protein sequence covered by the experimentally detected peptides.

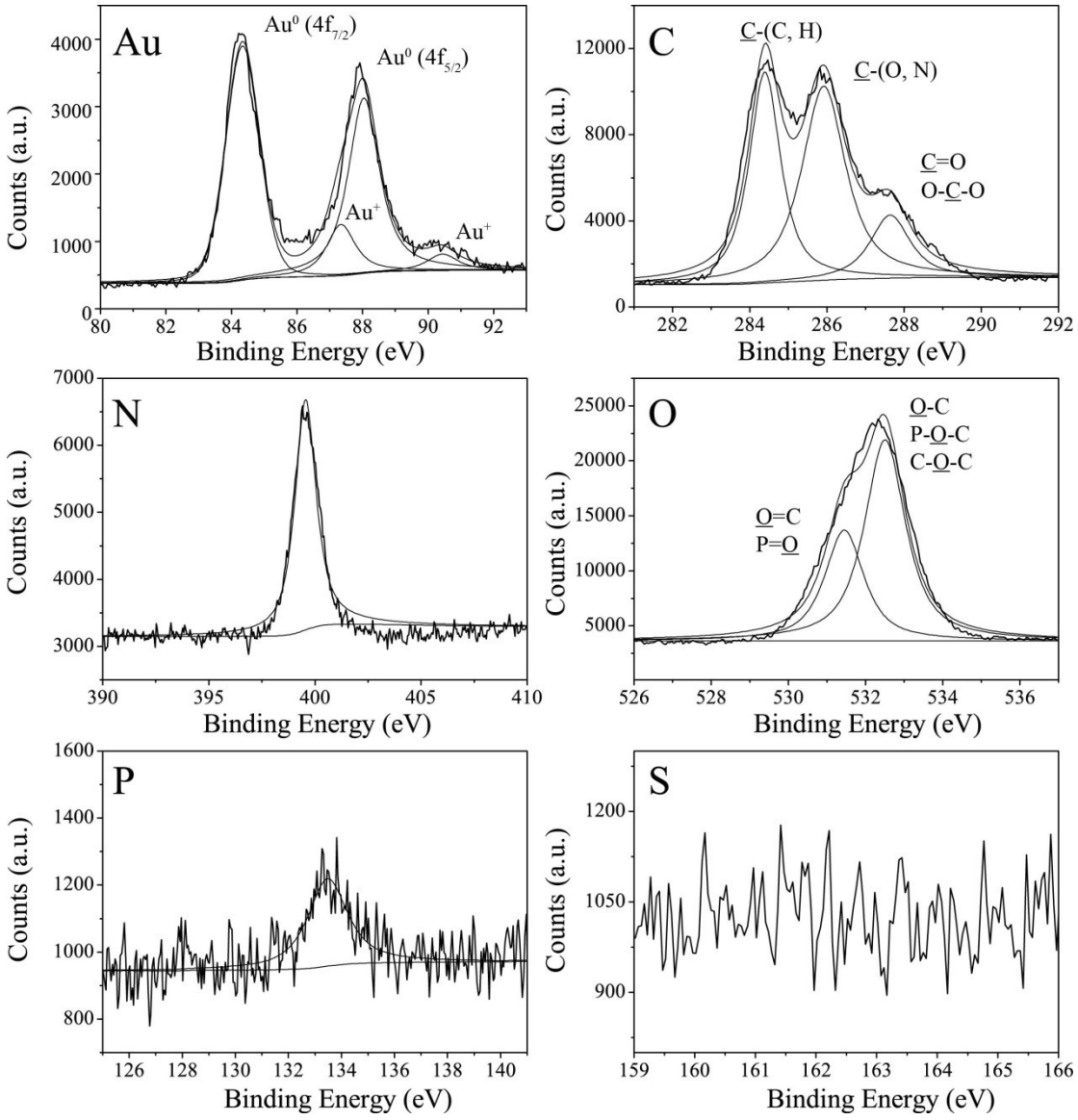


**Figure S3.** Au 4f, C1s, N1s, O1s, P2p, and S2p XPS spectra measured on the extracellular Au NPs. (The components of peak fitting in Au spectra were corresponded to $Au^0$ (84.3 and 87.9 eV) and $Au^+$ (87.3 and 90.4 eV))

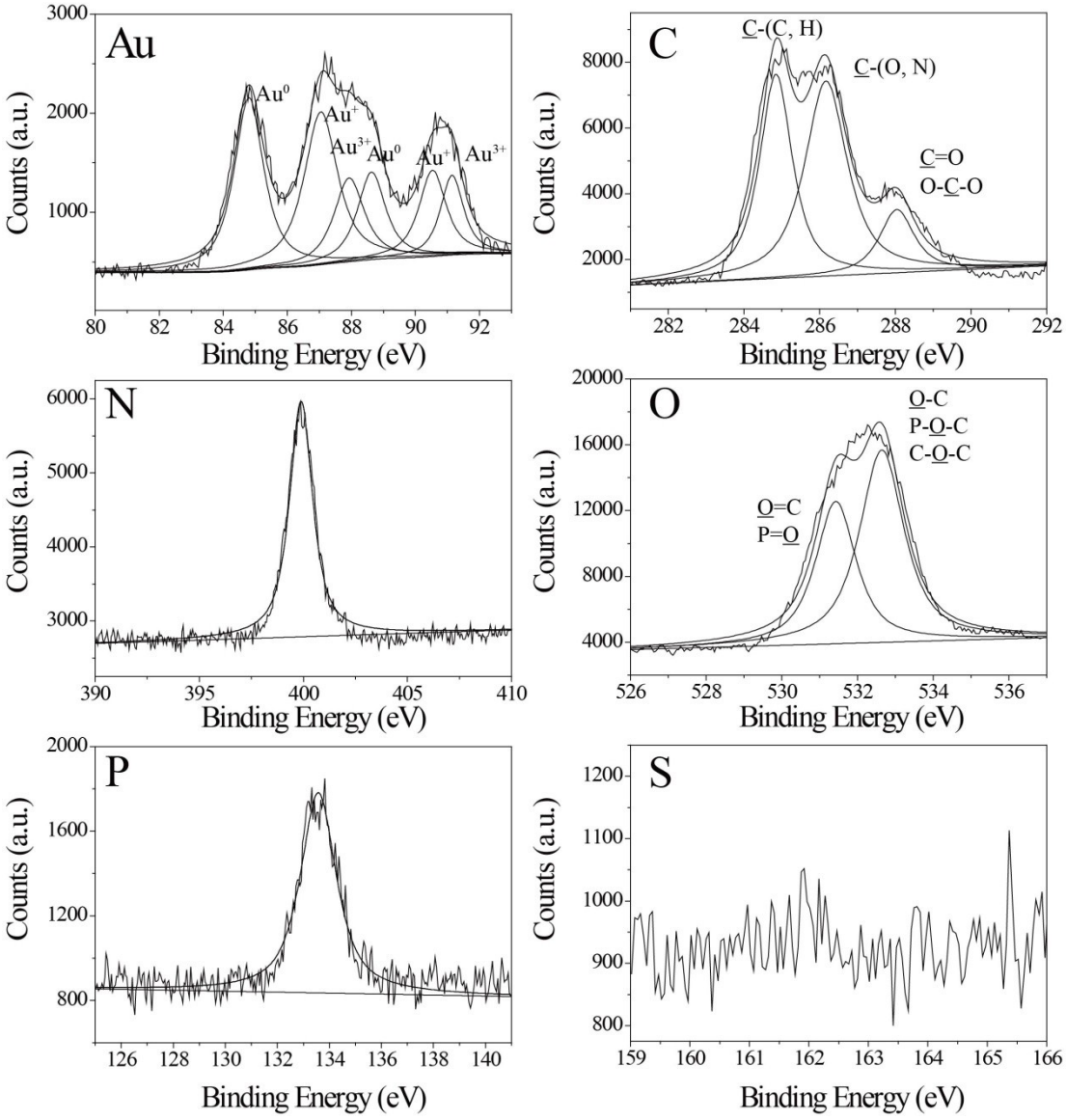


**Figure S4.** Au 4f, C1s, N1s, O1s, P2p, and S2p XPS spectra measured on the intracellular Au NPs. (The components of peak fitting in Au spectra were corresponded to $Au^0$ (84.8 and 88.4 eV), $Au^+$ (87.3 and 90.4 eV), and $Au^{3+}$ (87.9 and 91.1 eV))

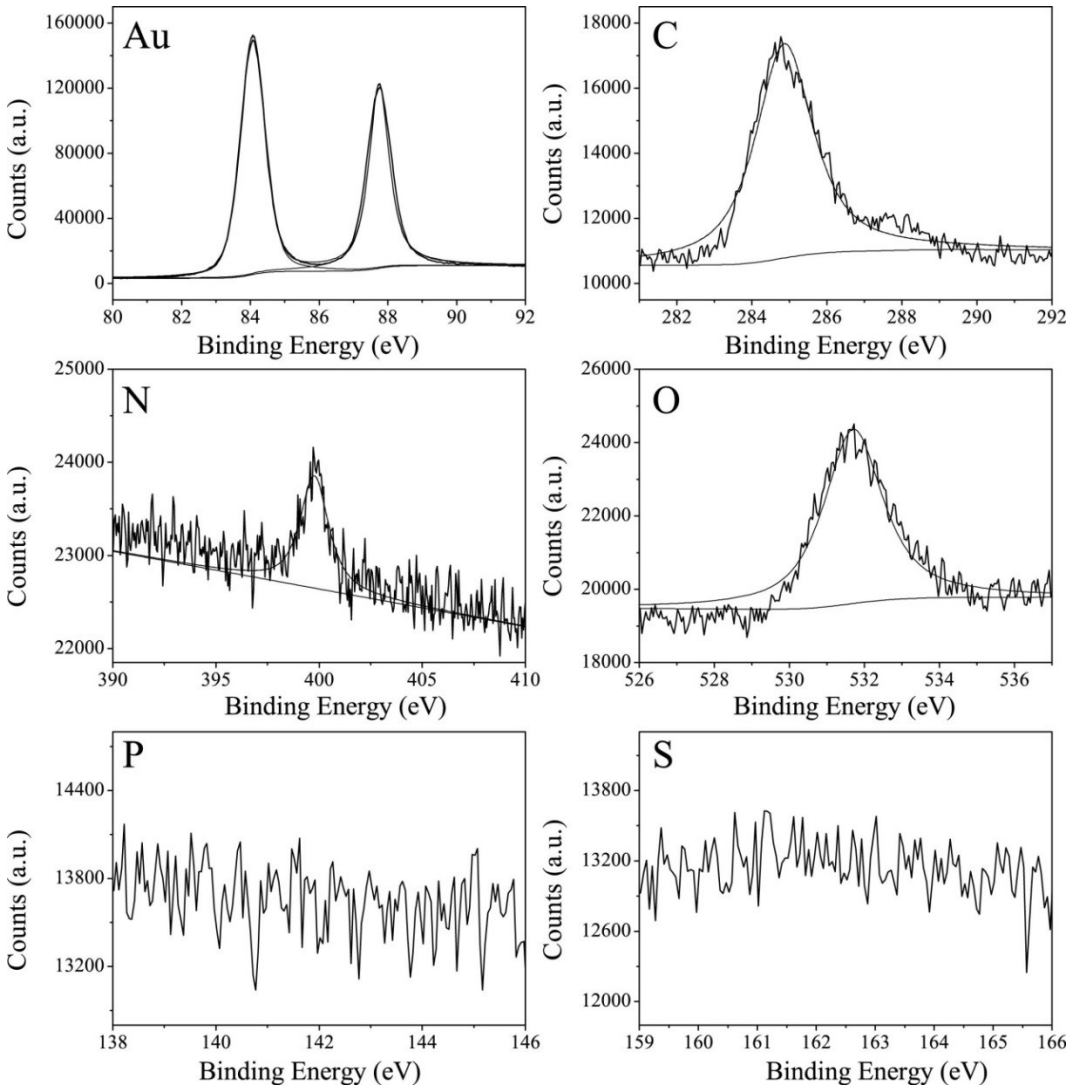


**Figure S5.** Au 4f, C1s, N1s, O1s, P2p, and S2p XPS spectra measured on the bare Au NPs(Control sample).

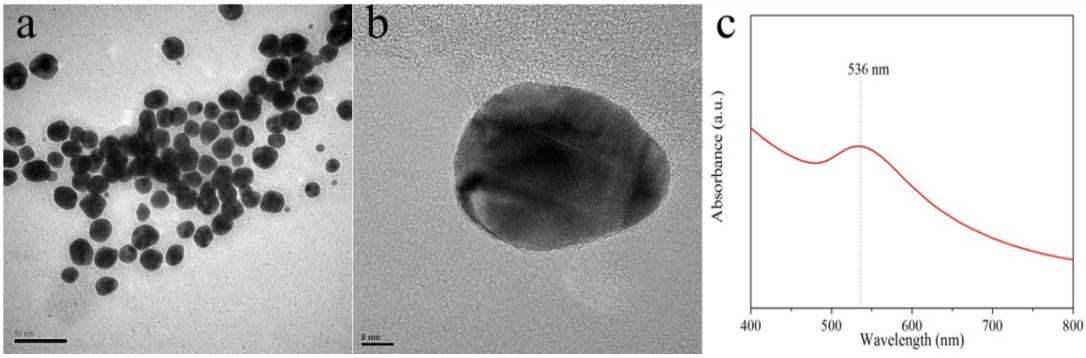


**Figure S6.** TEM images of Au NPs formed from Au(III) *in vitro* with aqueous EPS.

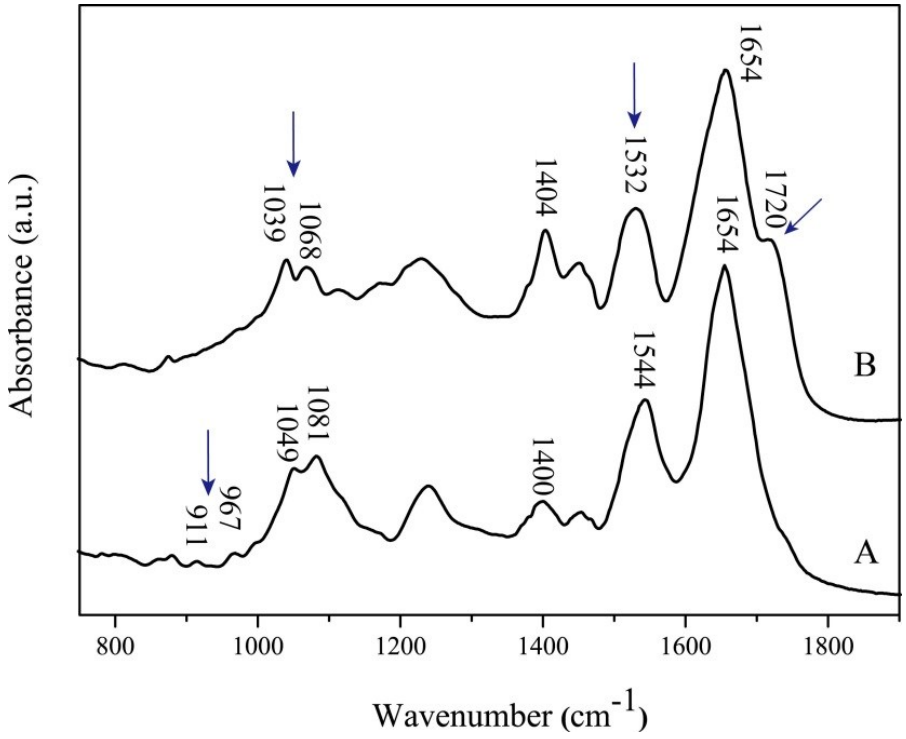


**Figure S7.** (A) Pristine EPS and (B) EPS reacted with Au(III)

**Table S5.** Assignment of peaks in FTIR spectra of pristine EPS (A) and EPS reacted with Au(III)(B) (Figure S7)[35-37].

| **Wavenumbers ($cm^{-1}$) A** | **Wavenumbers ($cm^{-1}$) B** | **Peak assignment** |
|---|---|---|
| | 1720 | C=O stretching in lipid and triglycerides |
| 1654 | 1654 | C=O stretching (amide I) |
| 1544 | 1532 | N−H bending and C−N stretching (amide II), $COO^-$ asymmetric stretching. |
| 1453 | 1453 | $CH_2$ bending in lipids |
| 1400 | 1404 | $COO^-$ symmetric stretching in carboxylate |
| 1240 | 1233 | $PO_2^-$ asymmetric stretching |
| 1081 | 1068 | $PO_2^-$ stretching |
| 1049 | 1039 | P-O-C twisting |
| 967 | | $C\text{-}N^+\text{-}C$ stretching |
| 911 | | C-O-C stretching |
| 879 | 879 | $NO_2$ symmetric stretching |
| 860 | | $PO_2^-$ symmetric twisting vibration |

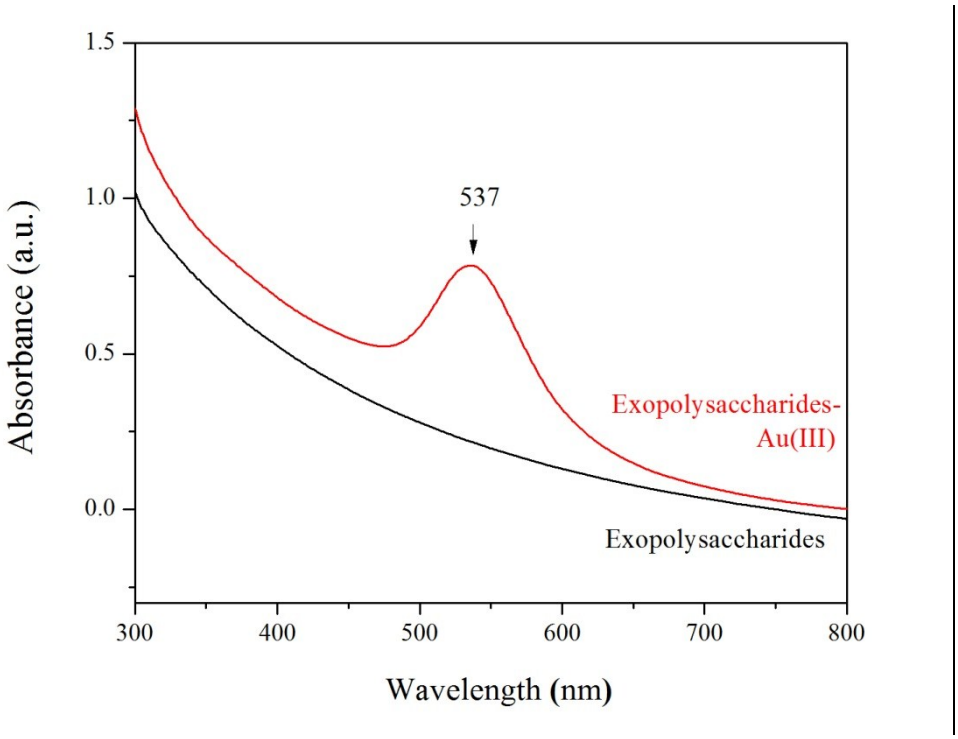


**Figure S8**. UV-Vis spectra of exopolysaccharides and exopolysaccharides reacted with Au(III).

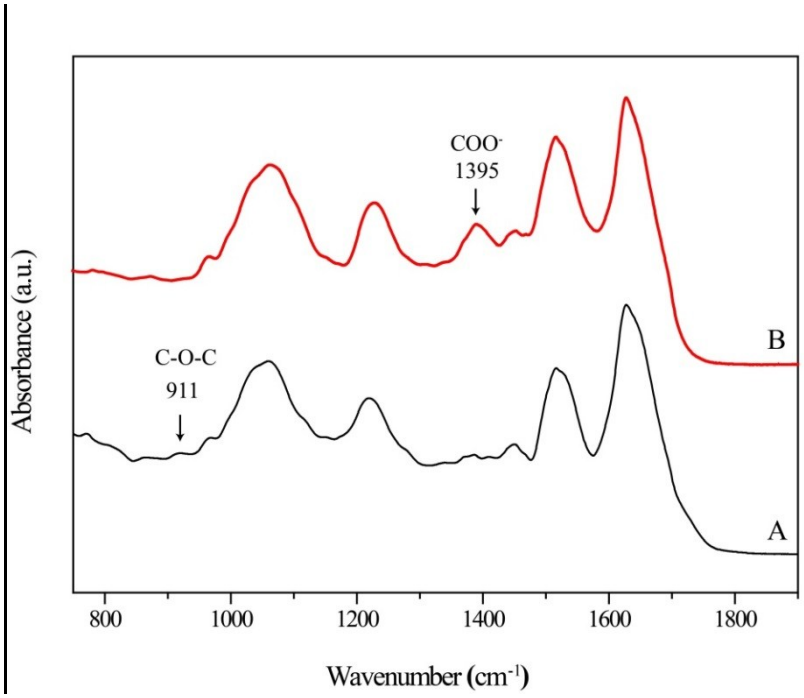


**Figure S9**. FTIR spectra of (A) exopolysaccharides, and (B) exopolysaccharides reacted with Au(III).

When exopolysaccharides were incubated with 2 mM Au(III) for 12 hours, a UV-vis peak at ~ 537 nm was observed due to the surface plasmon resonance (SPR) of Au

NPs (Figure S8), confirming that exopolysaccharides can chemically reduce Au(III) to Au NPs in the EPS. Meanwhile, FTIR spectra of exopolysaccharides before and after Au(III) incubation were collected to identify the functional groups in Au(III) reduction, and the results are shown in Figure S9. The spectrum of exopolysaccharides is similar that of EPS (Figure S7), suggesting that exopolysaccharides are an important component in the EPS.

Notably, after exopolysaccharides reacted with Au(III), a new peak was resolved at 1395 $cm^{-1}$, which is ascribed to $COO^-$ symmetric stretching;[38] whereas the band at 911 $cm^{-1}$, assigned to C-O-C stretching of acetal group,[39] was disappeared. This change in the C-O bands in exopolysaccharides was the same as in the EPS (Figure S7), confirming that exopolysaccharides is the specific biological component as the reducing agent in the EPS.

The reaction pathway is detailed as follows [40]:

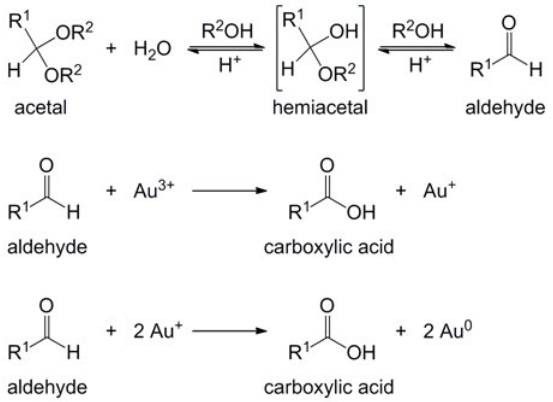


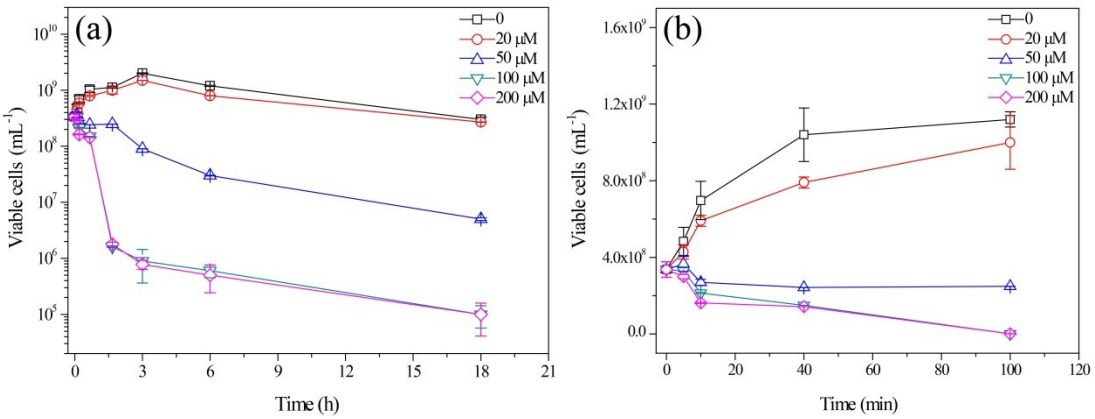


**Figure S10.** Cells change in PBS buffer with the Au(III) concentration and duration time

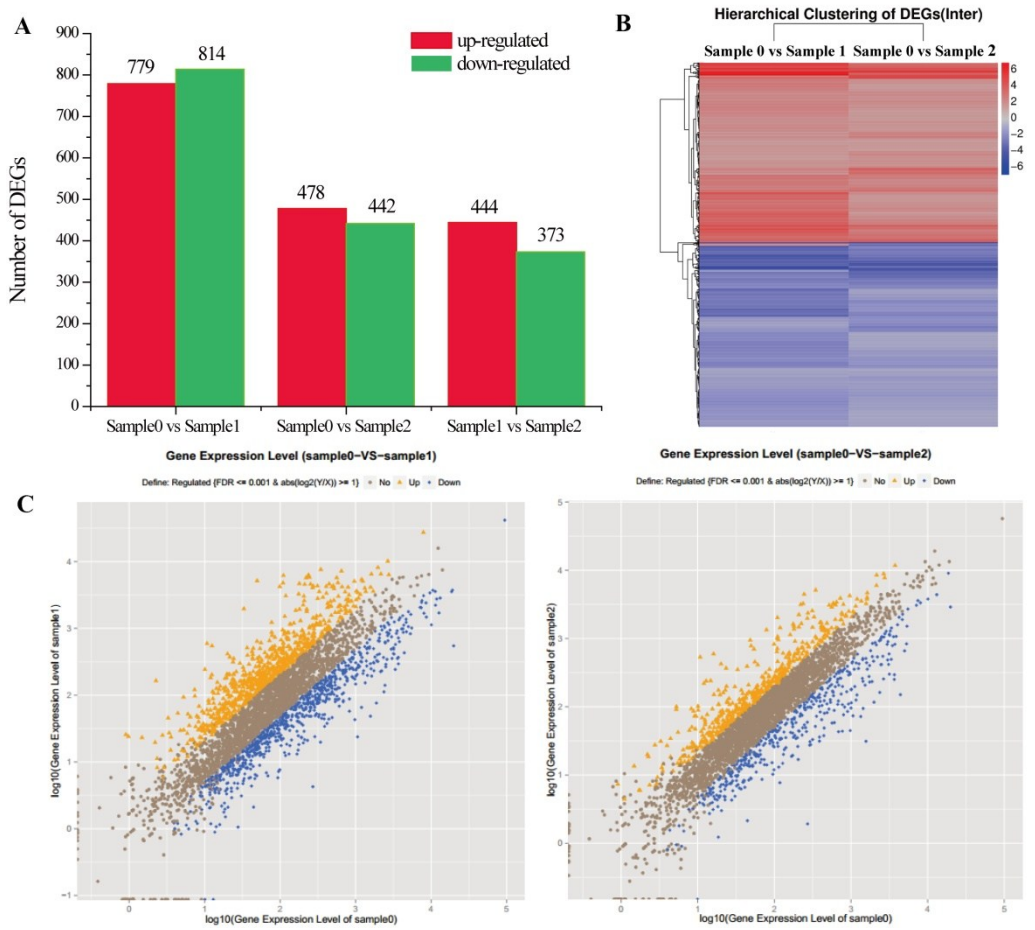


**Figure S11.** Sample0: no induction time; Sample1: with Au(III) for 10 min induction; Sample2: with Au(III) for 35 min induction. (A) Statistic chart of differently expressed genes. (B) The Hierarchical Clustering of the differentially expressed genes (DEGs) under Au(III) (Sample0 vs Sample1) vs Control (Sample0 vs Sample 2). Color scale shows log2 signal intensity values. (C) Differential gene expression by *Pantoea* sp. IMH (sample0 vs sample1) and (sample0 vs sample2).

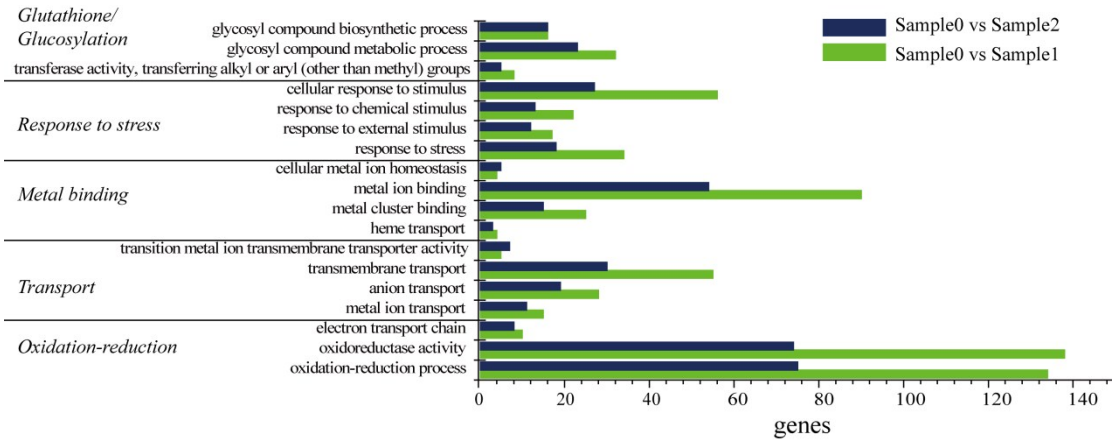


**Figure S12.** Gene Ontology (GO) functional annotation of differentially expressed genes (DEGs) in *Pantoea* sp. IMH.

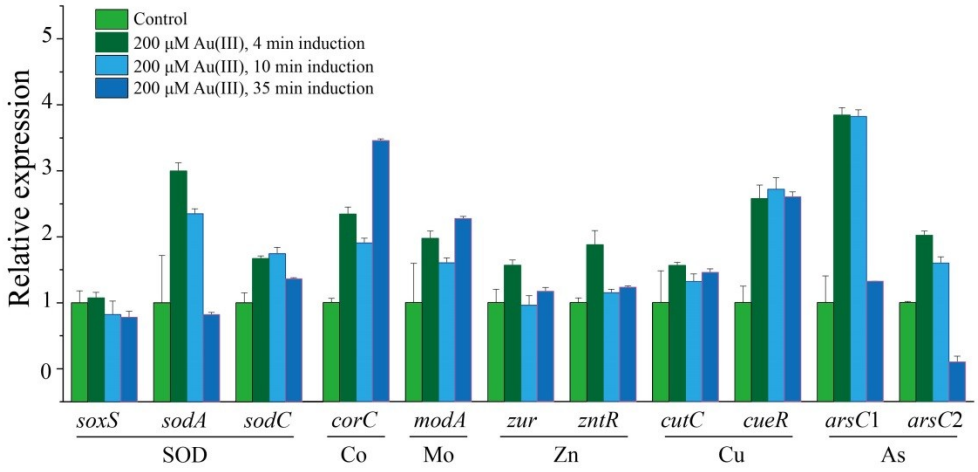


**Figure S13.** Q-PCR of differentially expressed genes in *Pantoea* sp. IMH.

**Table S6**. The annotation of genes in our study.

| Gene | Annotation |
|---|---|
| *fucO* | lactaldehyde reductase |
| *TC.PIT* | inorganic phosphate transporter, PiT family |
| *gloB* | Glutathione metabolism: hydroxyacylglutathione hydrolase |
| *soxR* | MerR family transcriptional regulator, redox-sensitive transcriptional activator SoxR |
| *soxS* | AraC family transcriptional regulator, transcriptional activator of the superoxide response regulon |
| *soxA* | superoxide dismutase, Fe-Mn family |
| *soxC* | Cu/Zn superoxide dismutase |
| *cueO* | blue copper oxidase |
| *copA* | $Cu^{2+}$-exporting ATPase |
| *cutC* | copper homeostasis protein |
| *cueR* | MerR family transcriptional regulator, copper efflux regulator |
| *arsC* | arsenate reductase |
| *zntR* | MerR family transcriptional regulator, Zn(II)-responsive regulator of zntA |
| *zur* | Fur family transcriptional regulator, zinc uptake regulator |
| *znuB* | zinc transport system permease protein |
| *feoB* | ferrous iron transport protein B, which involved in the cobalt export process. |
| *corC* | magnesium and cobalt transporter |
| *modA* | molybdate transport system substrate-binding protein |

**Table S7.** Sequences of oligonucleotide primers used for real-time RT-PCR

| **Primer** | **Gene** | **Oligoncleotide primer sequence (5′—3′)** |
|---|---|---|
| *soxS-F* | *soxS* | CGACTGGATCGAAGAGA |
| *soxS-R* | *soxS* | GCAAACTGACGGCGAAATAC |
| *sodA-F* | *sodA* | TCACTACCATCCCTGCCTTA |
| *sodA-R* | *sodA* | CCAGAAGAAGCTGTGGTTAGAG |
| *sodC-F* | *sodC* | CGCAGACCAAAGAGGGTAAA |
| *sodC-R* | *sodC* | GGCTCATCGGCATGGTTAT |
| *corC-F* | *corC* | CTGGTCACGATTGAGGACATTC |
| *corC-R* | *corC* | TCGGCCATAGCAACCTTAAAC |
| *modA-F* | *modA* | CGATCAGCAGTGGATGGATTAT |
| *modA-R* | *modA* | CAGGCACCCAGACTTTGTAA |
| *zur-F* | *zur* | TTCTGCTGGAACAGGGATTC |
| *zur-R* | *zur* | CATCGCAATCACGGCATAATC |
| *zntR-F* | *zntR* | TGATGGATCATGAGGTTCGC |
| *zntR-R* | *zntR* | ATAGCGTTCACTTCACTCAGAC |
| *cutC-F* | *cutC* | GTCGCTTTCCTTCGTGAACT |
| *cutC-R* | *cutC* | CAATCCACTTTCGGCACTCT |
| *cueR-F* | *cueR* | AAGAGTGTCGCGAGATGATTAG |
| *cueR-R* | *cueR* | TTTCTGCAGATGCCGTATGA |
| *arsC1-F* | *arsC1* | CCGTCACGATCTATCACAACC |
| *arsC1-R* | *arsC1* | TTCAATCAGTGCGGGATGG |
| *arsC2-F* | *arsC2* | GAGCCGACCGTTATTCATTATCT |
| *arsC2-R* | *arsC2* | GAACATCCAGCACGACTTCA |

**References**

1. Buré, C.; Ayciriex, S.; Testet, E.; Schmitter, J. M. A Single Run LC-MS/MS Method for Phospholipidomics. *Anal. Bioanal. Chem.* **2013**, *405*, 203-213.

2. Dai, L.; Kang, G.; Li, Y.; Nie, Z.; Duan, C.; Zeng, R. In-depth Proteome Analysis of the Rubber Particle of Hevea Brasiliensis (Para Rubber Tree). *Plant Mol. Biol*. **2013**, *82*, 155-168.

3. Ravel, B.; Newville, M. Athena, Artemis, Hephaestus: Data Analysis for X-ray Absorption Spectroscopy Using IFEFFIT. *J.Synchrotron. Radiat.* **2005**, *12*, 537−541.

4. Cui, J.; Shi, J.; Jiang, G.; Jing, C. Arsenic Levels and Speciation from Ingestion Exposures to Biomarkers in Shanxi, China: Implications for Human Health. *Environ. Sci. Technol.* **2013**, *47*, 5419−5424.

5. Kang, F. X.; Alvarez, P. J.; Zhu, D. Q., Microbial Extracellular Polymeric Substances Reduce Ag+ to Silver Nanoparticles and Antagonize Bactericidal Activity. *Environ. Sci. Technol.* **2014**, *48*, 316-322.

6. Shao, L. I.; Wu, Z.; Zhang, H.; Chen, W.; Ai, L.; Guo, B, Partial characterization and immunostimulatory activity of exopolysaccharides from Lactobacillus rhamnosus KF5. *Carbohyd. Polym.* **2014**, *107*, 51-56.

7. Guo, L.; Han, L.; Yang, L.; Zeng, H.; Fan, D.; Zhu, Y.; Zhou, D. Genome and Transcriptome Analysis of the Fungal Pathogen Fusarium oxysporum f. sp. cubense causing Banana Vascular Wilt Disease. *PLoS One* **2014**, *9*, e95543.

8. Bullard, J. H.; Purdom, E.; Hansen, K. D.; Dudoit, S. Evaluation of Statistical Methods for Normalization and Differential Expression in mRNA-Seq experiments. *BMC Bioinf.* **2010**, *11*, 94.

9. Chen, S.; Yang, P.; Jiang, F.; Wei, Y.; Ma, Z. De novo Analysis of Transcriptome Dynamics in the Migratory Locust during the Development of Phase Traits. *PLoS One* **2010**, *5*, e15633.

10. Livak, K. J.; Schmittgen, T. D. Analysis of Relative Gene Expression Data using Real-time Quantitative PCR and the 2−ΔΔCT method. Methods, 2001; pp 402–408.

11. Beveridge, T. J.; Murray, R. G. E., Sites of Metal-Deposition in the Cell-Wall of *Bacillus* subtilis. *J. Bacteriol.* **1980,** *141*, 876-887.

12. Lengke, M. F.; Fleet, M. E.; Southam, G., Morphology of Gold Nanoparticles Synthesized by Filamentous Cyanobacteria from Gold(I)-thiosulfate and Gold(III)-chloride Complexes. *Langmuir* **2006,** *22*, 2780-2787.

13. Reith, F.; Rogers, S. L.; McPhail, D. C.; Webb, D., Biomineralization of Gold: Biofilms on Bacterioform Gold. *Science* **2006,** *313*, 233-236.

14. He, S.; Guo, Z.; Zhang, Y.; Zhang, S.; Gu, J. W., Biosynthesis of Gold Nanoparticles Using the Bacteria *Rhodopseudomonas capsulata*. *Mater. Lett.* **2007,** *61*, 3984-3987.

15. Reith, F.; Etschmann, B.; Grosse, C.; Moors, H.; Benotmane, M. A.; Monsieurs, P.; Grass, G.; Doonan, C.; Vogt, S.; Lai, B.; Martinez-Criado, G.; George, G. N.; Nies, D. H.; Mergeay, M.; Pring, A.; Southam, G.; Brugger, J., Mechanisms of Gold Biomineralization in the Bacterium Cupriavidus metallidurans. *Proc. Natl. Acad. Sci. U. S. A.* **2009,** *106*, 17757-17762.

16. Kalishwaralal, K.; Deepak, V.; Pandian, S. R. K.; Kottaisamy, M.; BarathManiKanth, S.; Kartikeyan, B.; Gurunathan, S., Biosynthesis of Silver and Gold Nanoparticles Using Brevibacterium casei. *Colloids Surf., B* **2010,** *77*, 257-262.

17. Konishi, Y.; Tsukiyama, T.; Tachimi, T.; Saitoh, N.; Nomura, T.; Nagamine, S., Microbial Deposition of Gold nanoparticles by the Metal-reducing Bacterium Shewanella algae. *Electrochim. Acta* **2007,** *53*, 186-192.

18. Focsan, M.; Ardelean, I. I.; Craciun, C.; Astilean, S., Interplay between Gold Nanoparticle Biosynthesis and Metabolic Activity of cyanobacterium Synechocystis sp PCC 6803. *Nanotechnology* **2011,** *22*,

19. Ravindranath, S. P.; Henne, K. L.; Thompson, D. K.; Irudayaraj, J., Raman Chemical Imaging of Chromate Reduction Sites in a Single Bacterium Using Intracellularly Grown Gold Nanoislands. *Acs Nano* **2011,** *5*, 4729-4736.

20. Arunkumar, P.; Thanalakshmi, M.; Kumar, P.; Premkumar, K., Micrococcus Luteus Mediated Dual Mode Synthesis of Gold Nanoparticles: Involvement of Extracellular Alpha-amylase and Cell wall teichuronic acid. *Colloids Surf., B* **2013,** *103*, 517-522.

21. Girilal, M.; Fayaz, A. M.; Balaji, P. M.; Kalaichelvan, P. T., Augmentation of PCR Efficiency Using Highly Thermostable Gold Nanoparticles Synthesized from a Thermophilic bacterium, Geobacillus stearothermophilus. *Colloids Surf., B* **2013,** *106*, 165-169.

22. Johnston, C. W.; Wyatt, M. A.; Li, X.; Ibrahim, A.; Shuster, J.; Southam, G.; Magarvey, N. A., Gold Biomineralization by a Metallophore from a Gold-Associated Microbe. *Nat. Chem. Biol.* **2013,** *9*, 241-243.

23. Varia, J. C.; Zegeye, A.; Velasquez-Orta, S.; Bull, S., Process Analysis of AuCl4-Sorption Leading to Gold Nanoparticle Synthesis by Shewanella putrefaciens. *Chem. Eng. J.* **2016,** *288*, 482-488.

24. Srivastava, S. K.; Yamada, R.; Ogino, C.; Kondo, A., Biogenic Synthesis and Characterization of Gold Nanoparticles by Escherichia coli K12 and Its Heterogeneous Catalysis in Degradation of 4-nitrophenol. *Nanoscale Res. Lett.* **2013,** *8*, 70.

25. Govindaraju, K.; Basha, S. K.; Kumar, V. G.; Singaravelu, G., Silver, Gold and Bimetallic Nanoparticles Production Using Single-cell Protein (Spirulina platensis) Geitler. *J. Mater. Sci.* **2008,** *43*, 5115-5122.

26. Lengke, M.; Southam, G., Bioaccumulation of Gold by Sulfate-reducing Bacteria Cultured in the Presence of Gold(I)-thio Sulfate Complex. *Geochim. Cosmochim. Acta* **2006,** *70*, 3646-3661.

27. Kalishwaralal, K.; Deepak, V.; Pandian, S. R. K.; Gurunathan, S., Biological Synthesis of Gold Nanocubes from Bacillus licheniformis. *Bioresour. Technol.* **2009,** *100*, 5356-5358.

28. Feng, Y.; Yu, Y.; Wang, Y.; Lin, X., Biosorption and Bioreduction of Trivalent Aurum by Photosynthetic Bacteria Rhodobacter capsulatus. *Curr. Microbiol.* **2007,** *55*, 402-408.

29. Wen, L.; Lin, Z.; Gu, P.; Zhou, J.; Yao, B.; Chen, G.; Fu, J., Extracellular Biosynthesis of Monodispersed Gold Nanoparticles by a SAM Capping Route. *J. Nanopart. Res.* **2009,** *11*, 279-288.

30. Du, L.; Jiang, H.; Liu, X.; Wang, E., Biosynthesis of Gold Nanoparticles Assisted by Escherichia coli DH5 alpha and Its application on Direct Electrochemistry of Hemoglobin. *Electrochem. Commun.* **2007,** *9*, 1165-1170.

31. Nair, B.; Pradeep, T., Coalescence of Nanoclusters and Formation of Submicron Crystallites Assisted by Lactobacillus strains. *Cryst. Growth Des.* **2002,** *2*, 293-298.

32. Severin, A.; Nickbarg, E.; Wooters, J.; Quazi, S. A.; Matsuka, Y. V.; Murphy, E.; Moutsatsos, I. K.; Zagursky, R. J.; Olmsted, S. B., Proteomic Analysis and Identification of Streptococcus Pyogenes Surface-Associated Proteins. *J. Bacteriol.* **2007**, *189*, 1514-1522.

33. Xu, M.; Bijoux, H.; Gonzalez, P.; Mounicou, S., Investigating the Response of Cuproproteins from Oysters (Crassostrea gigas) after Waterborne Copper Exposure by Metallomic and Proteomic Approaches. *Metallomics* **2014**, *6*, 338-346.

34. Bateman, A.; Martin, M. J.; O'Donovan, C.; Magrane, M.; Apweiler, R.; Alpi, E.; Antunes, R.; Arganiska, J.; Bely, B.; Bingley, M.; Bonilla, C.; Britto, R.; Bursteinas, B.; Chavali, G.; Cibrian-Uhalte, E.; Da Silva, A.; De Giorgi, M.; Dogan, T.; Fazzini, F.; Gane, P. *et al.*, UniProt: a Hub for Protein Information. *Nucleic Acids Res.* **2015**, *43*, D204-D212.

35. Schmitt, J.; Flemming, H. C., FTIR-Spectroscopy in Microbial and Material Analysis. *Int. Biodeterior. Biodegrad.* **1998**, *41*, 1-11.

36. Bosch, A.; Minan, A.; Vescina, C.; Degrossi, J.; Gatti, B.; Montanaro, P.; Messina, M.; Franco, M.; Vay, C.; Schmitt, J.; Naumann, D.; Yantorno, O., Fourier Transform Infrared Spectroscopy for Rapid Identification of Nonfermenting Gram-negative Bacteria Isolated from Sputum Samples from Cystic Fibrosis Patients. *J. Clin. Microbiol.* **2008**, *46*, 2535-2546.

37. Fischer, G.; Braun, S.; Thissen, R.; Dott, W., FT-IR Spectroscopy as a Tool for Rapid Identification and Intra-Species Characterization of Airborne Filamentous Fungi. *J. Microbiol. Methods* **2006**, *64*, 63-77.

38. Maquelin, K.; Kirschner, C.; Choo-Smith, L. P.; van den Braak, N.; Endtz, H. P.; Naumann, D.; Puppels, G. J., Identification of medically relevant microorganisms by vibrational spectroscopy. *J. Microbiol. Methods* **2002**,*51*, 255-271.

39. Movasaghi, Z.; Rehman, S.; ur Rehman, D. I., Fourier transform infrared (FTIR) spectroscopy of biological tissues. *Appl. Spectrosc. Rev.* **2008**, *43*, 134-179.

40. Kang, F.; Qu, X.; Alvarez, P. J.; Zhu, D., Extracellular saccharide-mediated reduction of Au3+ to gold nanoparticles: new insights for heavy metals biomineralization on microbial surfaces. *Environmental science & technology Environ. Sci. Technol.* **2017**,*51*, 2776-2785.